Università di Napoli "Federico II"

Fluidodinamica Numerica

Ingegneria Aerospaziale

Double Driven Cavity flow with oscillating lids

Author:
A. CAROTENUTO

Supervisor:
Prof. G. Coppola

Academic Year 2023-2024

Abstract

The aim of this paper is to study the flow dynamic inside a cavity when both the upper and lower lid oscillate at different frequencies. We look for the combination of frequencies that optimizes the 'mixing'. The study of this particular aspect is carried out by tracking the position of a finite number of flow particles through time. The same observations are repeated for different Reynolds numbers.So numerical simulations of the 2D lid-driven cavity are performed using staggered grid based finite differences method.

1 Introduction

The lid-driven cavity problem has been deeply investigated over the years and has served for the development of ever more reliable and efficient methods to numerically solve the Navier-Stokes equations. Today a wide variety of articles and papers assessing different aspects of this problem is available. Particularly noteworthy is the article by Ghia *et al.* [1] on the two dimensional driven cavity problem for high Reynolds numbers, or the results made available by the experimental investigation of Koseff *et al.* [2] on the end wall effects. Recently, the research has extended to the study of the effects of oscillating lids on the cavity flow. Indukuri *et al.* [3] in particular have investigated the case of parallel and anti-parallel wall oscillations. In the pursuit of a deeper understanding of the problem studied by Indukuri we have examined a wider range of configurations by taking into account the effects of parallel oscillating lids at different frequencies. Particular attention has been given to the ability of these oscillations to influence the 'mixing' of the fluid inside the cavity, trying to identify the configuration that maximizes this phenomenon. The effects of Reynolds number have also been taken into account. The simulations have been performed with Reynolds numbers ranging from 500 to 5,000.

2 Mathematical and Numerical approach

2.1 Fractional step method

The code has been designed for the solution of Navier-Stokes 2D equations in primitive variables, here presented in nondimensional form:

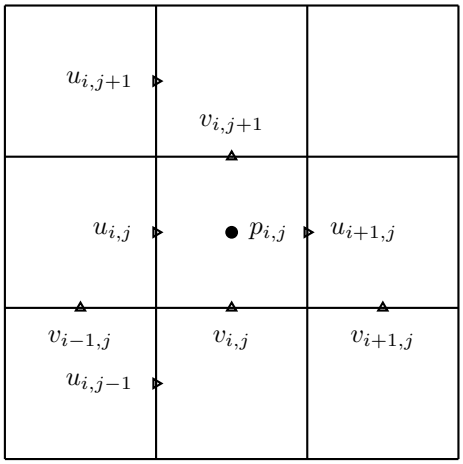

Figure 1: Harlow-Welch staggering in 2D

$$\nabla \cdot \mathbf{V} = 0 \tag{1}$$

$$\frac{\partial \mathbf{V}}{\partial t} = -\mathbf{V} \cdot \nabla \mathbf{V} + \frac{1}{\mathrm{Re}} \nabla^2 \mathbf{V} - \nabla p \, . \tag{2}$$

Where V is the Velocity V = (u, v) and p is the modified pressure. We proceed by using a classic fractional step method on a Harlow-Welch staggered mesh (Fig. 1).

First, through the spatial discretization of the advective and diffusive terms, we find V^* such that

$$\frac{\partial \mathbf{V}^*}{\partial t} = -\mathbf{V} \cdot \nabla \mathbf{V} + \frac{1}{\mathrm{Re}} \nabla^2 \mathbf{V} \tag{3}$$

and then we identify the value of p whose gradient corrects the divergence of V^* so that (1) is verified:

$$\nabla \cdot \frac{\partial \mathbf{V}}{\partial t} = \nabla \cdot \frac{\partial \mathbf{V}^*}{\partial t} - \nabla^2 p = 0 \tag{4}$$

$$\frac{\partial \mathbf{V}}{\partial t} = \frac{\partial \mathbf{V}^*}{\partial t} - \nabla p \tag{5}$$

We evolve the solution through time with a Runge-Kutta fourth order scheme. The Butcher array in Table 1 is used.

$$
\begin{array}{c|cccc}
 & & & & \\
0.5 & & & & \\
0 & 0.5 & & & \\
0 & 0 & 1 & & \\
\hline
\frac{1}{6} & \frac{1}{3} & \frac{1}{3} & \frac{1}{6}
\end{array}
$$

Table 1: Butcher array for Runge-Kutta scheme.

2.2 Boundary conditions

The flow dynamics inside the cavity depends on the oscillating movements of the upper and lower lids. Equations (6) and (7) define the horizontal velocity of the lids.

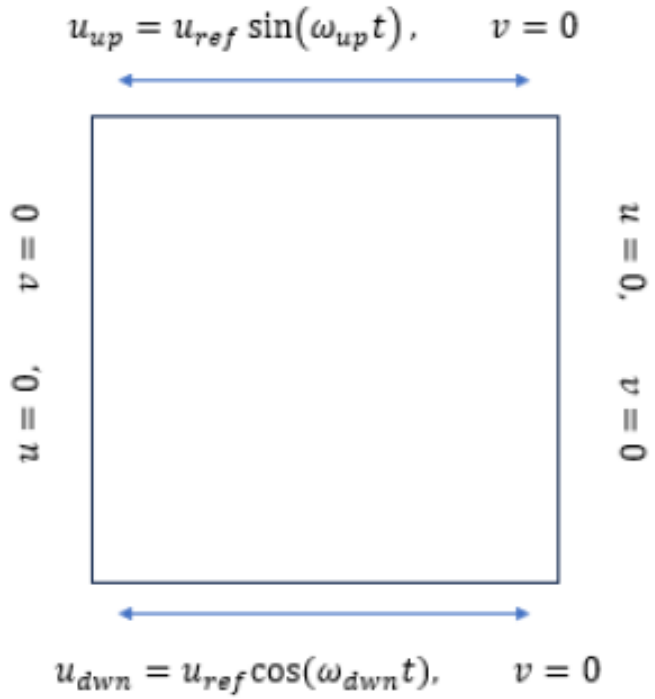

Figure 2: Boundary Conditions for velocity components.

$$u_{up}(t) = u_{ref} \sin \omega_{up} t \tag{6}$$
$$u_{dwn}(t) = u_{ref} \cos \omega_{dwn} t \tag{7}$$

The diagram in (Fig. 2) shows the Boundary conditions for velocity on each wall. The purpose of this study is to observe the behavior of the fluid for different combinations of ω_{up} and ω_{dwn}. The way we decided to approach this task is to set ω_{up} equal to a reference value

$$\omega_{up} = \omega_{ref} \tag{8}$$

and then define the parameter K as follows:

$$K = \frac{\omega_{dwn}}{\omega_{up}} \tag{9}$$

Substituting Eqs. (8) and (9) inside (6) and (7) we rewrite the boundary condition equations as

$$u_{up}(t) = u_{ref} \sin \omega_{ref} t \tag{10}$$
$$u_{dwn}(t) = u_{ref} \cos K\omega_{ref} t \tag{11}$$

By choosing different values for ω_{ref} for k=1 we change the frequency of the lower lid and the upper lid in the same way. Simulations have been carried out for values of ω_{ref}: 0.5, 0.8, 1, 1.2, 2. By choosing different values for K we change the frequency of the lowerlid oscillations with respect to the upper lid. Simulations have been carried out for values of K: 0, 0.3, 1, 2, 5.

2.3 'Mixing' properties

In order to evaluate the influence that K and Re have on the mixing of the fluid we follow the path of a finite number of particles initially concentrated at the centre of the cavity. It takes more time to the vorticity to affect the centre of the cavity and there the motion of the particles is less influenced by the presence of the wall. If L_x and L_y are the width and height of the cavity respectively, the initial positions of the nine particles are the ones shown in

Fig. 3:

x_0	y_0
$\frac{9}{20}L_x$	$\frac{9}{20}L_y$
$\frac{10}{20}L_x$	$\frac{9}{20}L_y$
$\frac{11}{20}L_x$	$\frac{9}{20}L_y$
$\frac{9}{20}L_x$	$\frac{10}{20}L_y$
$\frac{10}{20}L_x$	$\frac{10}{20}L_y$
$\frac{11}{20}L_x$	$\frac{10}{20}L_y$
$\frac{9}{20}L_x$	$\frac{11}{20}L_y$
$\frac{10}{20}L_x$	$\frac{11}{20}L_y$
$\frac{11}{20}L_x$	$\frac{11}{20}L_y$

(12)

In order to draw the pathline of each particle, (13) needs to be solved. We integrate through time with the same Runge-Kutta scheme shown in Table 1.More specifically we use the same integration process for the parallel

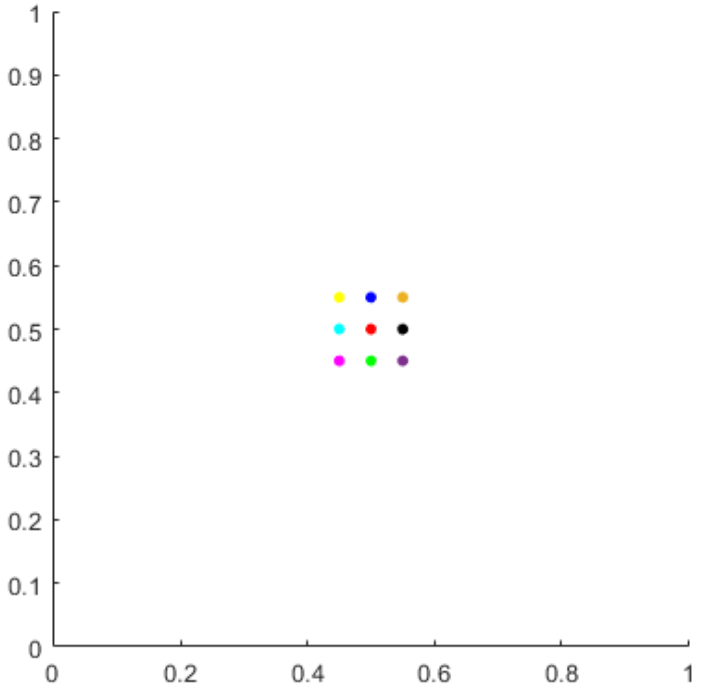

Figure 3: Particle positions at time 0.

solution of Eqs. (2) and (13). To clarify the meaning of the expression 'parallel solution' we look at the upgrade equation of x for the generic intermediate stage (14). It's easy to see that to obtain the position of the particle at time t^i (in our notation $\mathbf{x}^k = \mathbf{x}(t^k)$) we first need to find the discrete velocity at the previous stages $\underline{\mathrm{V}}^j = (U^j, V^j)$ and then interpolate on the position occupied by the particle x^j . Note that, at every timestep, only the end point of each pathline is plotted.

$$\frac{d\mathbf{x}}{dt} = \mathbf{V}(\mathbf{x}(t), t) \tag{13}$$

$$\mathbf{x}^i = \mathbf{x}^n + \sum_{j=1}^{i-1} a_{ij}\mathbf{V}(\mathbf{x}^j, t^j) \tag{14}$$

At this point we need to find an operational definition of 'dispersion' that allows us to evaluate how spread out or mixed the particles actually are. In this regard, we find that estimating the moment of inertia of the particle system, with respect to the centroid of said system, provides us with very useful information. If G is the centroid and I the moment of inertia, then by definition:

$$\mathrm{x_G} = \frac{\sum_{i=1}^{n} m_i \mathrm{x_i}}{\sum_{i=1}^{n} m_i} \tag{15}$$

$$I = \frac{\sum_{i=1}^{n} m_i |\mathrm{x_i} - \mathrm{x_G}|^2}{\sum_{i=1}^{n} m_i}. \tag{16}$$

Also, it's important to mention that the mass of every particle is assumed to be negligible so that the momentum does not influence the dynamic. If we label the moment of inertia of the initial configuration as I_0, we can define an index of dispersion:

$$i(t) = \frac{I(t)}{I_0} \tag{17}$$

i is evaluated at every timestep in order to determine how spread out the system of particles is with respect to the initial configuration.

2.4 Settings

The cavity is square with $L_x = L_y = 1$. The Mesh 80×80 is uniform along x and y axis. Every simulation is carried out for a total time of T=30. Although it was not explicitly required, the time interval Δt between each timestep happens to be always equal to $\Delta t = 0.0152$. Note that even though we solve Navier-Stokes equations for primary variables (that is to say for $\mathbf{V}$ and p) the results of the simulations are often reported in terms of the stream function ψ. This is defined in such a way that

$$u = \frac{\partial \psi}{\partial y}, \tag{18}$$

$$v = -\frac{\partial \psi}{\partial x} \tag{19}$$

Contour maps of the function are shown in which red lines are used to mark positive values of ψ and black lines are used for negative values.

3 Numerical results

3.1 Double driven cavity

Figures 4, 5, 6 show how the oscillations of the upper and lower lid affect the flow inside the cavity when Re = 2000 and K = 1 (both lids have the same frequency). The disturbance caused by the moving walls is first perceived near the walls themselves, but rapidly reaches the center of the cavity as we can already see. We can observe the formation of four primary vortices in proximity of the four corners of the cavity . These are of course caused by the alternate motion of the lids. We can see how each vortex is counter rotating with respect to the adjacent ones. This particular configuration appears to be somewhat stable at least with the combination of K and Re that we are presenting. Of course, being the lids neither parallel nor anti-parallel in their motion, we cannot observe the symmetries detectable in *et al.* [3].

3.2 Effects of frequency of the lower lid

Changes in the frequency of the oscillation of the lower lid primarily affect the vortex formation in the lower region of the cavity. In almost every case,

except K=0, we can observe a repeating pattern in the formation of four primary vortices near the corners. This formation generally appears by time t=10 s already. With the increase of K the vortices near the lower lid become vanishing and they easily dissipate as shown in Fig.11. The ones on the upper lid are instead scarcely affected by the change in K. We can still see the formation of the two primary vortices although they remain restricted to the upper portion of the cavity as they limit each other's penetration (resembling in fact the results for the single wall oscillation in *et al.* [3]). As a result, when K is higher, the central and lower regions are subject to very low disturbance, as it is possible to see in Fig.11, Fig.10. For K=5 the particles barely move

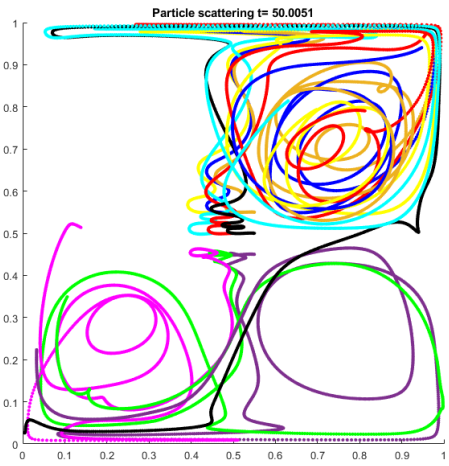

Figure 4: Particles' path for Re=2000, K=1 .

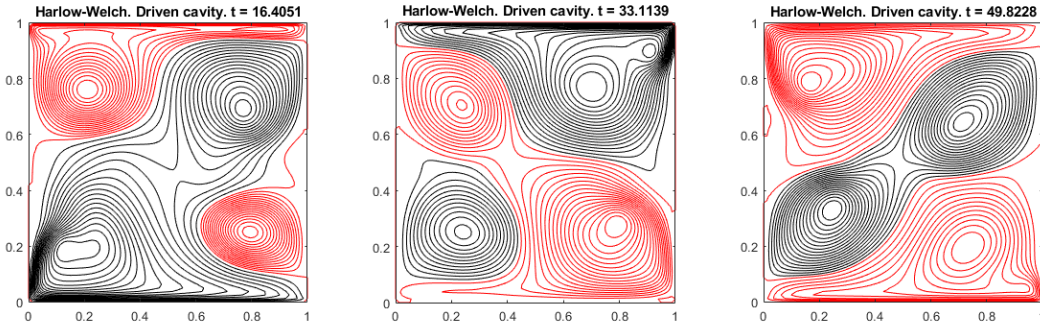

Figure 5: streamline for Re=2000, K=1 .

and up to t=20 only the ones closer to the upper lid move from their initial position. When K is less than 1, on the other hand, the frequency of the lower lid is less than that of the upper lid, which means that a longer time is required for the lower wall to reverse its motion. As a result the action of the lid on the fluid is carried out for a longer time interval and this allows for the formation of stronger vortices. It is not uncommon, when K is low, for two or more vortices to merge into a wider vortex, thus straying from the four vortices formation as shown in Fig. 8. For K=0 the lower wall is no longer oscillating and is in fact easy to see that u_{dwn}(t) =u_{ref}(t) . Since its velocity is uniform and steady only one vortex originates near the lower lid, rapidly reaching the upper region of the cavity. As we can see in Fig. 12 the case of K=0 is one where the particles rapidly move inside the cavity following the expansion of the primary vortex. However, the dispersion is not optimal as the particles still tend to remain close to each other in their motion.

3.3 Effects of Re

As it is well known, by altering the value of Re we are in fact varying the relative importance of convective and diffusive phenomena. As a consequence

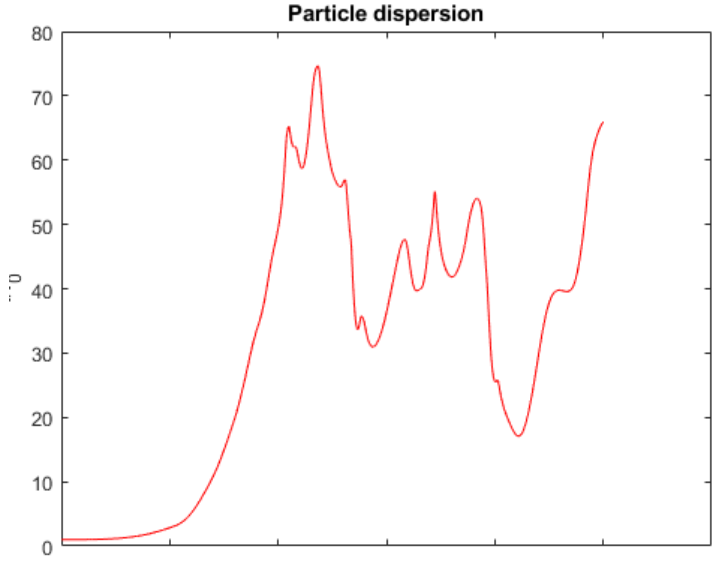

Figure 6: Mixing Index for Re=2000, K=1 .

of this, for lower values of Re we observe how vortices dissipate at a much higher rate compared to high Reynolds. As an example in Fig.18 and Fig.19 we show the case of Re=500 and Re=1000. We can easily notice how the primary vortices tend to decrease in size very rapidly when they are detached from the moving lid and how secondary vortices rapidly dissipate. Looking at Fig.21 we can instead see how, due to the lower viscosity, every vortex has a much higher persistence. It is very common to witness the formation of secondary vortices that oftentimes end up merging with bigger ones. The flow appears to be more chaotic when Re is higher this translate to a better mixing property as shown in Fig.26 .

3.4 Effects of ω_{ref}

With the increase of ω_{ref} a briefer time is required for the walls to reverse their motion . As a result the action of the lid on the fluid is carried out for a little time interval and this allows for the formation of weaker vortices (Fig.31). Thus when ω_{ref} is higher, the central regions are subject to very low disturbance, as it is possible to see in Fig. 36. For ω_{ref}=2 the particles barely move and up to t=20 only the ones closer to the lids move from their initial position. When ω_{ref} is less than 1, on the other hand, a longer time is required for the walls to reverse their motion. As a result the action of the lid on the fluid is carried out for a longer time interval and this allows for the formation of stronger vortices. It is not uncommon, when K is low, for two or more vortices to merge into a wider vortex, thus straying from the four vortices formation as shown in Fig. 27. However, the dispersion is not optimal as the particles still tend to remain close to each other in their motion.

4 Conclusions

When trying to maximize the dispersion of the particles inside the cavity we have seen (Fig. 17) how similar frequency values between the upper and lower lids (ranging from K=0.3 to K=2), grant consistently better results. We can also see that there is an high dispersion of particles for ω_{ref}=1 and it decreases if we consider higher or lower values for ω_{ref} as shown in 37. If we also take viscosity into account we can see that using a less viscous fluid (Re=5000) generally has a beneficial impact on particle dispersion (Fig. 26).

4.1 References

You should include references in your report. This can be done by using the `\cite{}` command. As an example, you can cite the article by Ghia *et al.* [1].

References

[1] U. Ghia, K. N. Ghia and C. T. Shin, *High-Re solutions for incompressible flow using the Navier-Stokes eq uations and a multigrid method*. Journal of Computational Physics **48**, 387-411 (1982).

[2] J. R. Koseff, A. K. Prasad, *Reynolds Number and end-wall effects on a lid-driven cavity flow Physics of Fluids A Fluid Dynamics*. **1**, 2 (1989).

[3] J. V. Indukuri, R. Maniyeri, *Numerical simulation of oscillating lid driven square cavity*. Alexandria Engineering Journal **57**, 2609–2625 (2018).

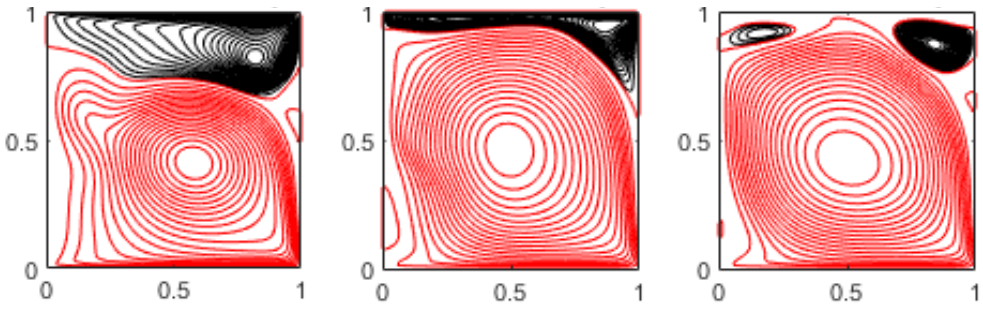

Figure 7: streamline for Re=2000, K=0 at 10, 20, 30 s.

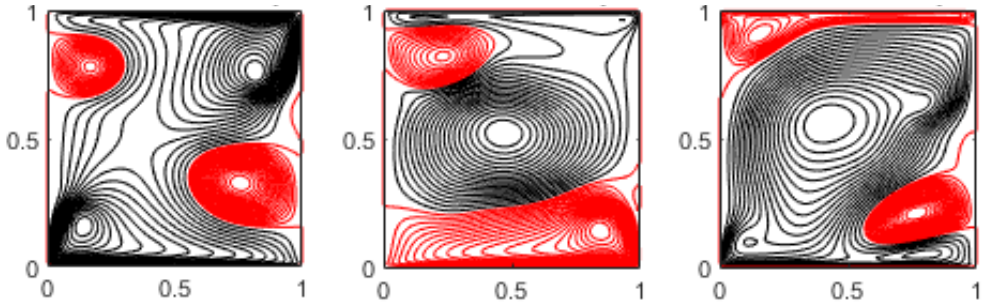

Figure 8: streamline for Re=2000, K=0.3 at 10, 20, 30 s.

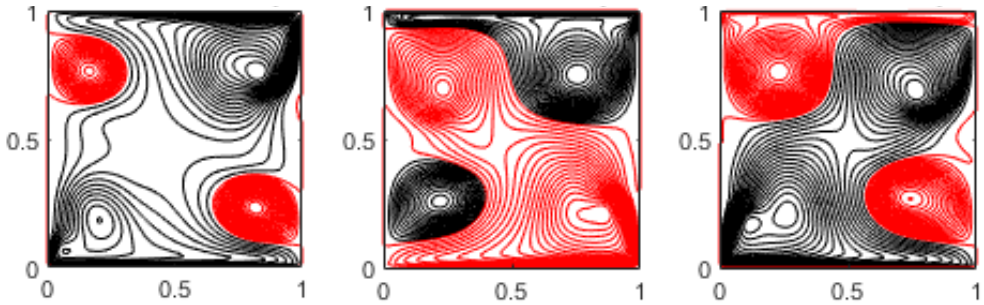

Figure 9: streamline for Re=2000, K=1 .

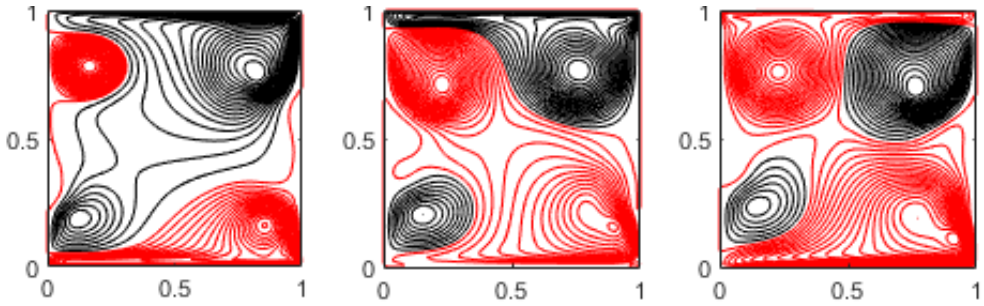

Figure 10: streamline for Re=2000, K=2 at 10, 20, 30 s.

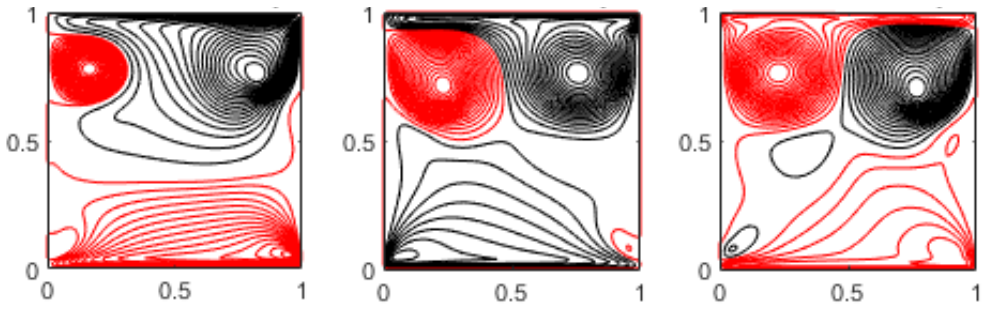

Figure 11: streamline for Re=2000, K=5 at 10, 20, 30 s.

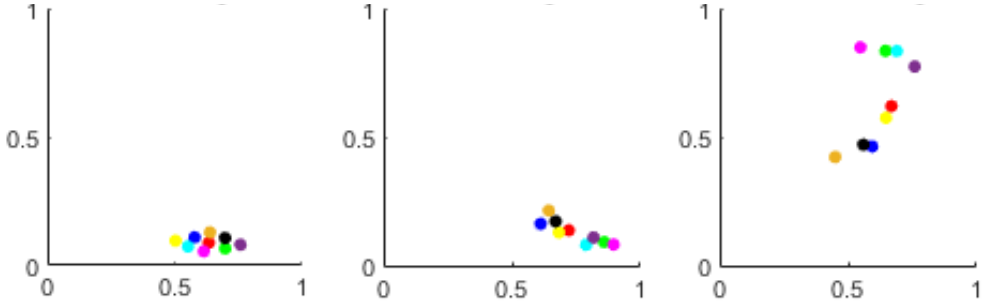

Figure 12: Particle position for Re=2000, K=0 at 10, 20, 30 s.

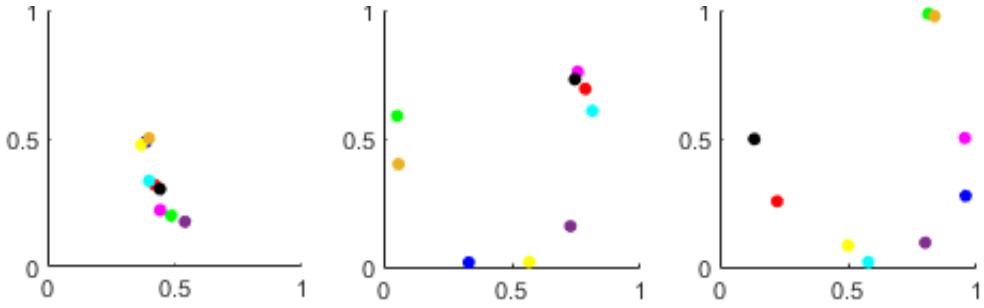

Figure 13: Particle position for Re=2000, K=0.3 at 10, 20, 30 s.

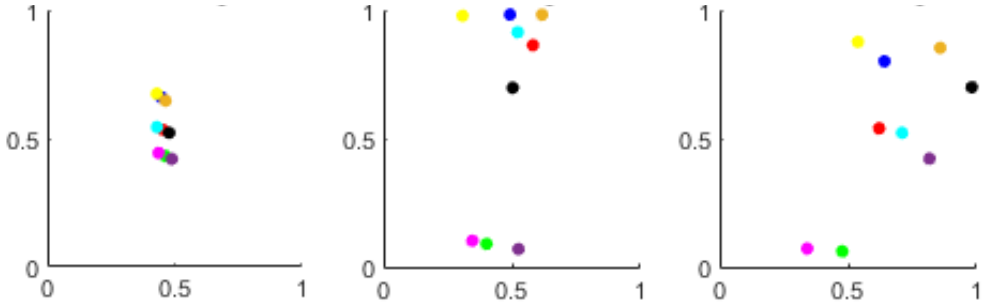

Figure 14: Particle position for Re=2000, K=1 at 10, 20, 30 s.

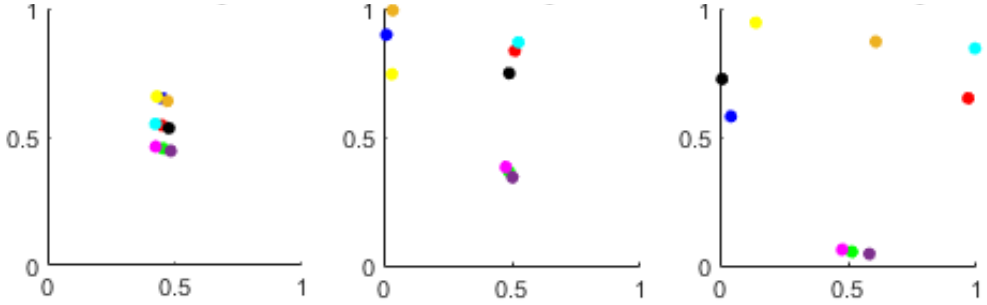

Figure 15: Particle position for Re=2000, K=2 at 10, 20, 30 s.

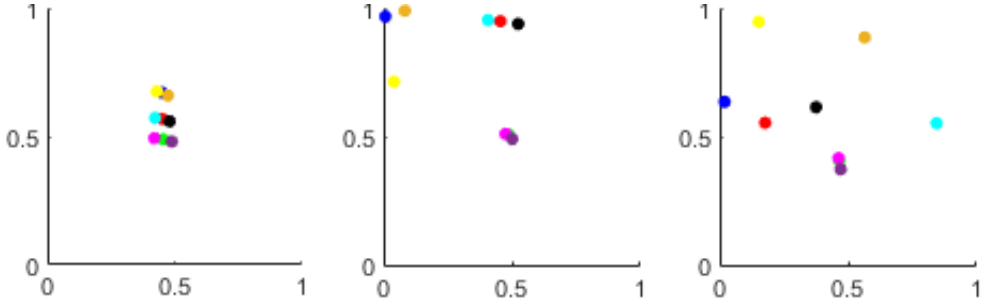

Figure 16: Particle position for Re=2000, K=5 at 10, 20, 30 s.

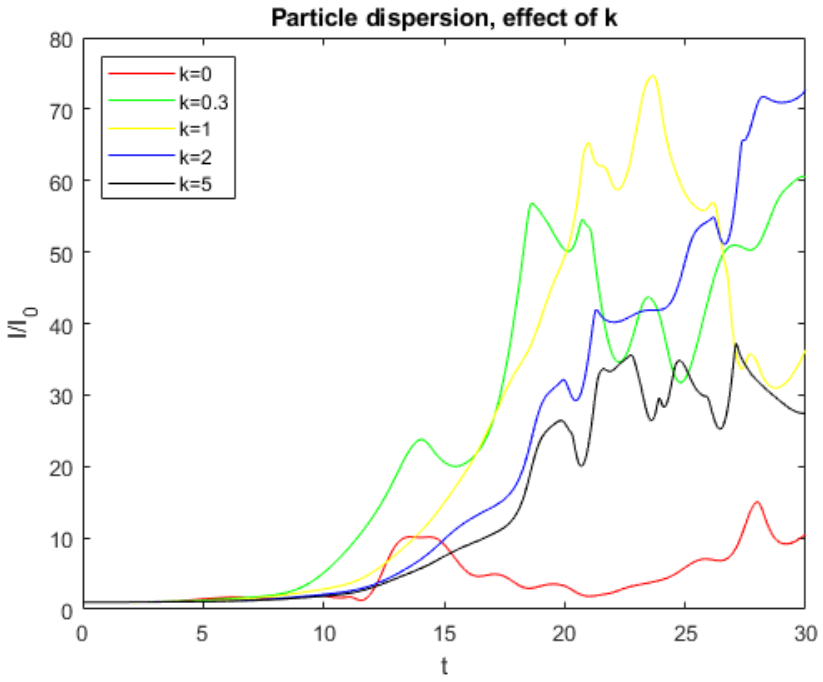

Figure 17: Indice di dispersione al variare di K.

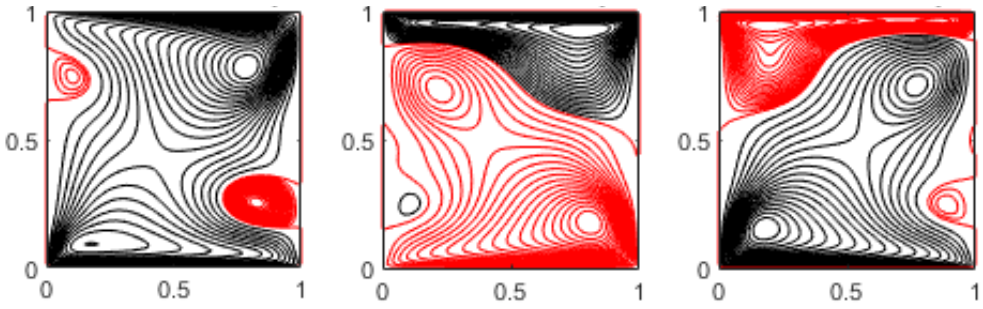

Figure 18: streamline for Re=500, K=1 at 10, 20, 30 s.

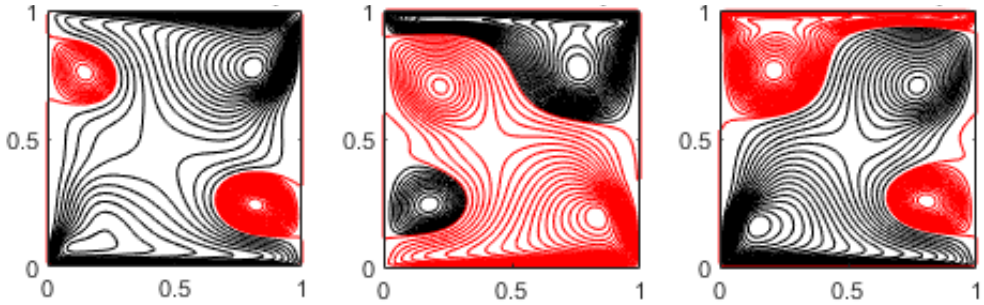

Figure 19: streamline for Re=1000, K=1 at 10, 20, 30 s.

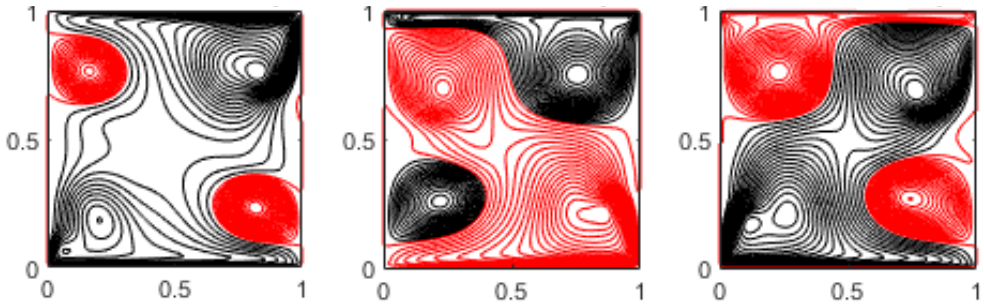

Figure 20: streamline for Re=2000, K=1 .

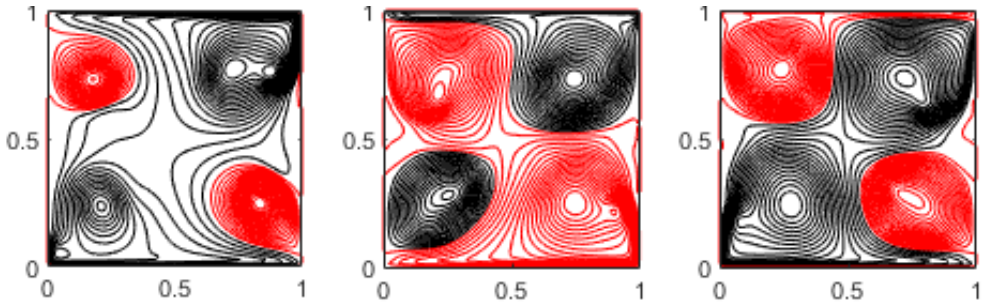

Figure 21: streamline for Re=5000, K=1 at 10, 20, 30 s.

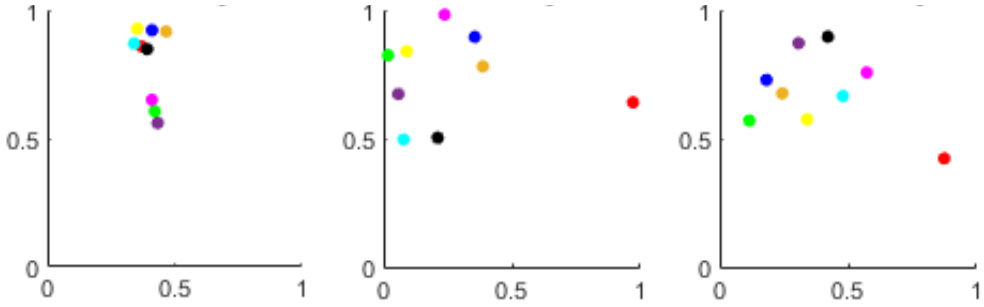

Figure 22: Particle position for Re=500, K=1 at 10, 20, 30 s.

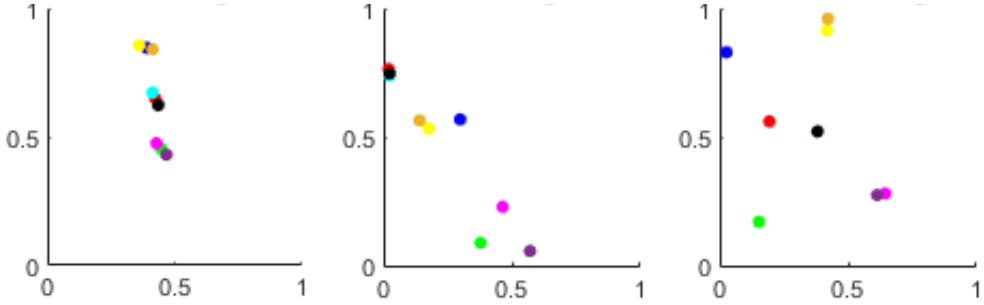

Figure 23: Particle position for Re=1000, K=1 at 10, 20, 30 s.

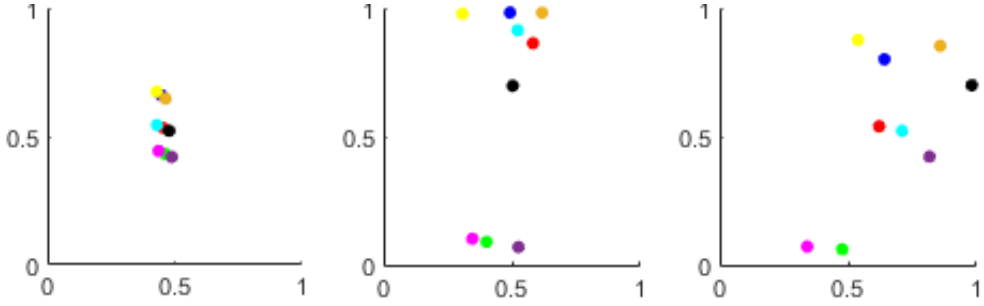

Figure 24: Particle position for Re=2000, K=1 at 10, 20, 30 s.

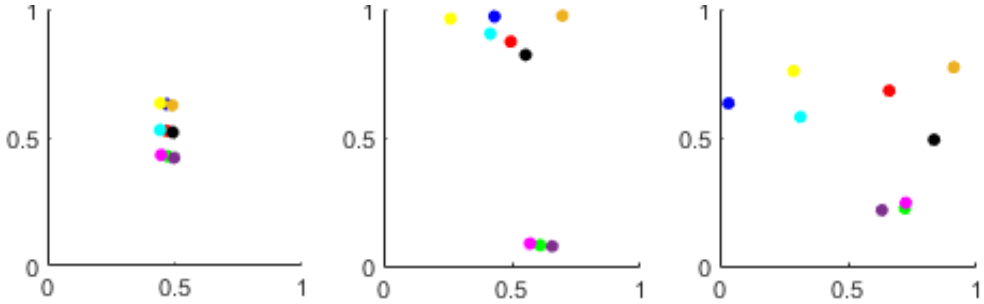

Figure 25: Particle position for Re=5000, K=1 at 10, 20, 30 s.

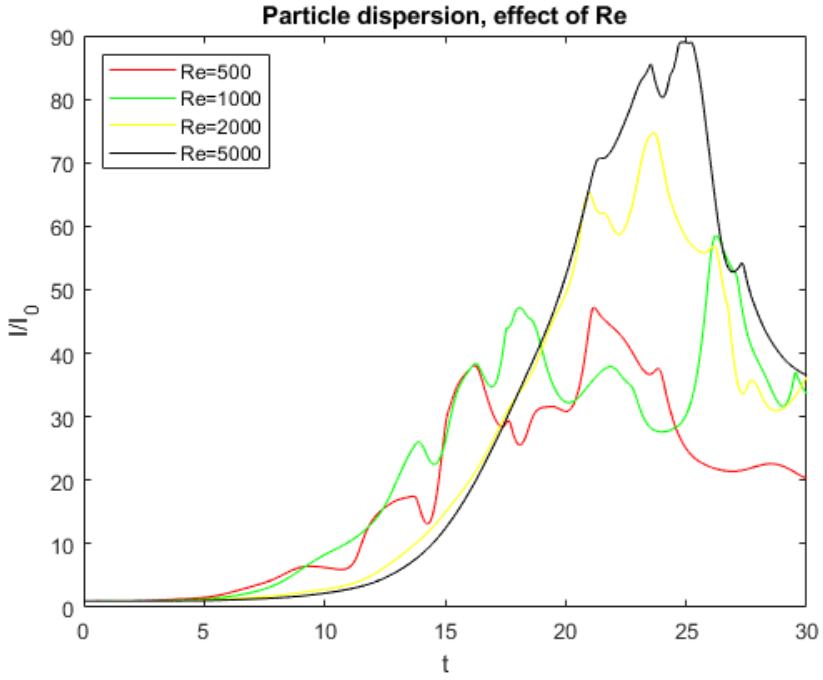

Figure 26: Indice di dispersione al variare di Re.

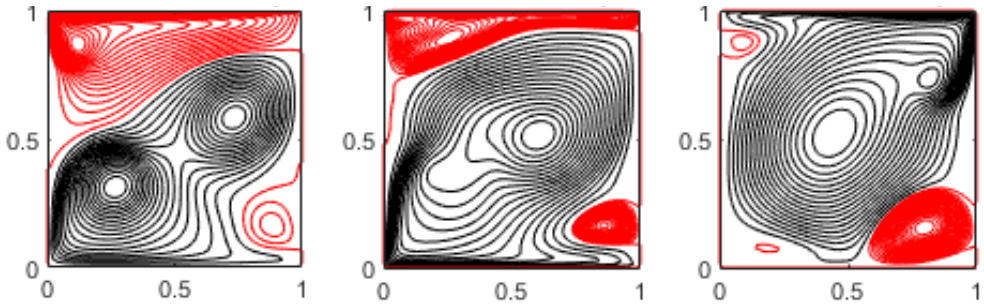

Figure 27: streamline for Re=2000, ω_{ref}=0.5 at 10, 20, 30 s.

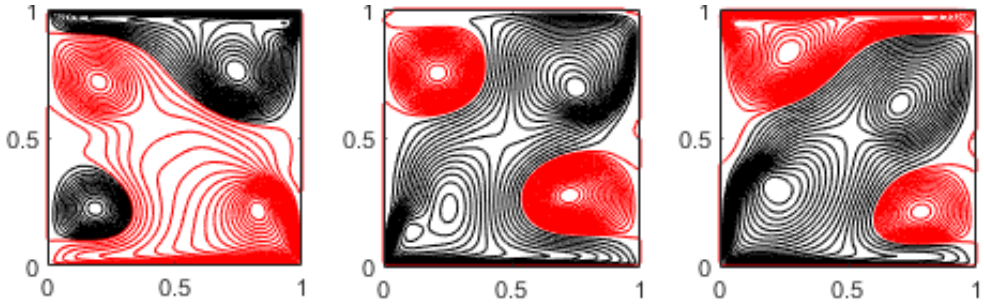

Figure 28: streamline for Re=2000, ω_{ref}=0.8 at 10, 20, 30 s.

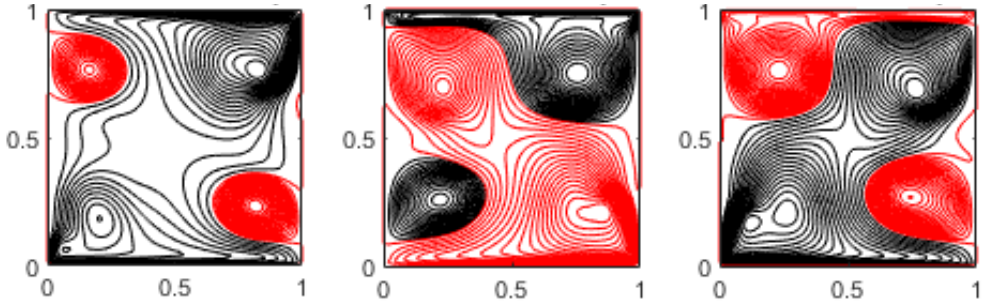

Figure 29: streamline for Re=2000, ω_{ref}=1 .

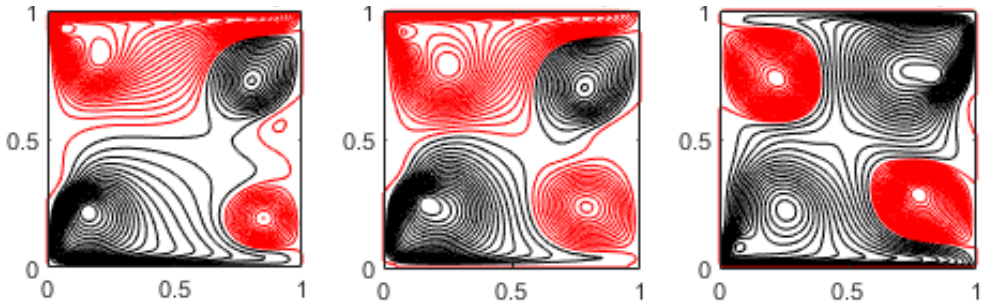

Figure 30: streamline for Re=2000, ω_{ref}=1.2 at 10, 20, 30 s.

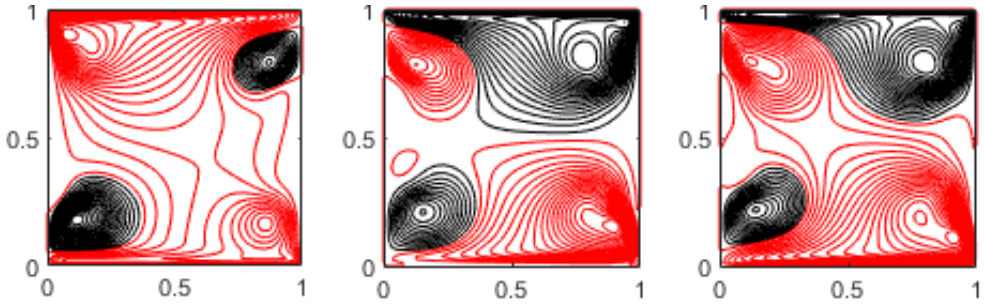

Figure 31: streamline for Re=2000, ω_{ref}=2 at 10, 20, 30 s.

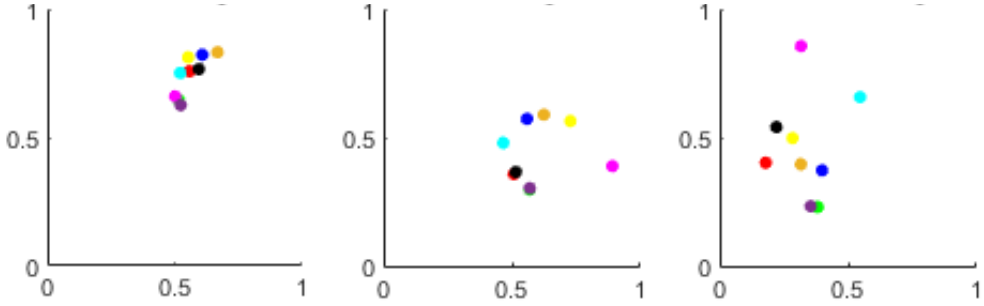

Figure 32: Particle position for Re=2000, ω_{ref}=0.5 at 10, 20, 30 s.

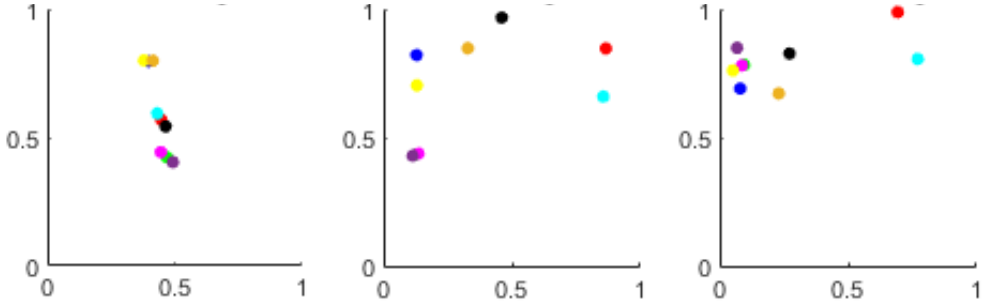

Figure 33: Particle position for Re=2000, ω_{ref}=0.8 at 10, 20, 30 s.

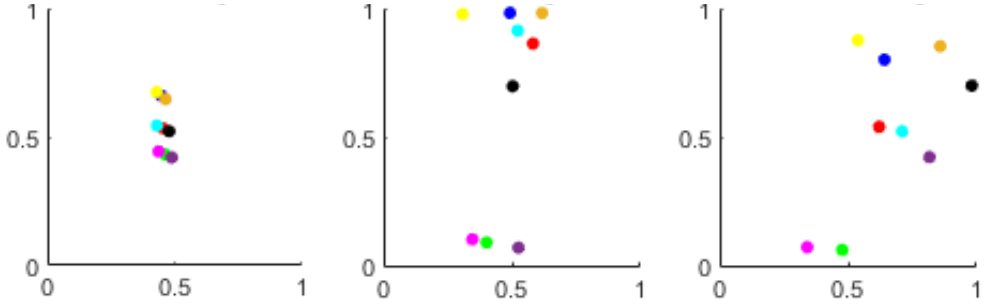

Figure 34: Particle position for Re=2000, K=1 at 10, 20, 30 s.

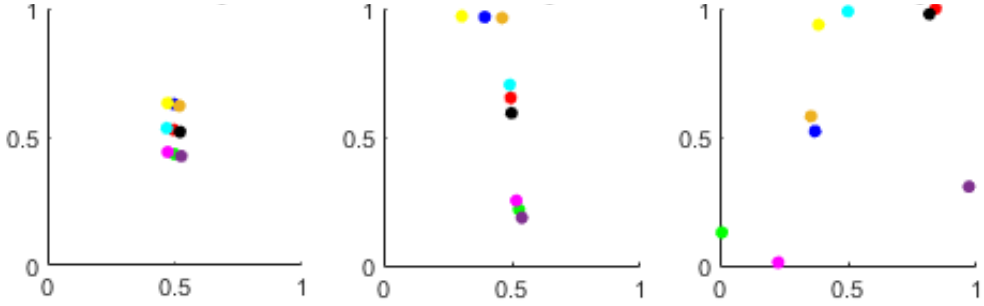

Figure 35: Particle position for Re=2000, ω_{ref}=1.2 at 10, 20, 30 s.

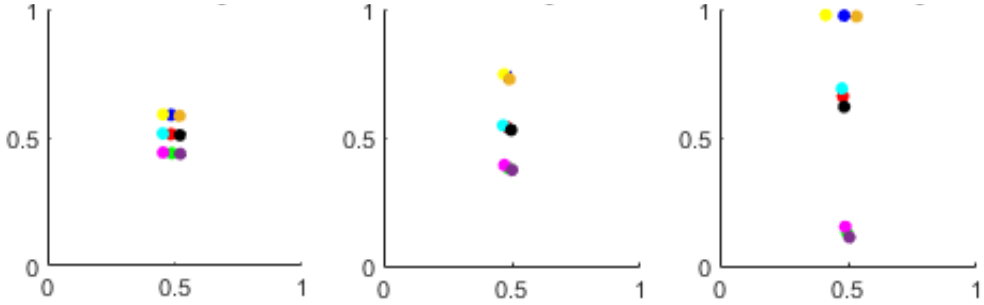

Figure 36: Particle position for Re=2000, ω_{ref}=2 at 10, 20, 30 s.

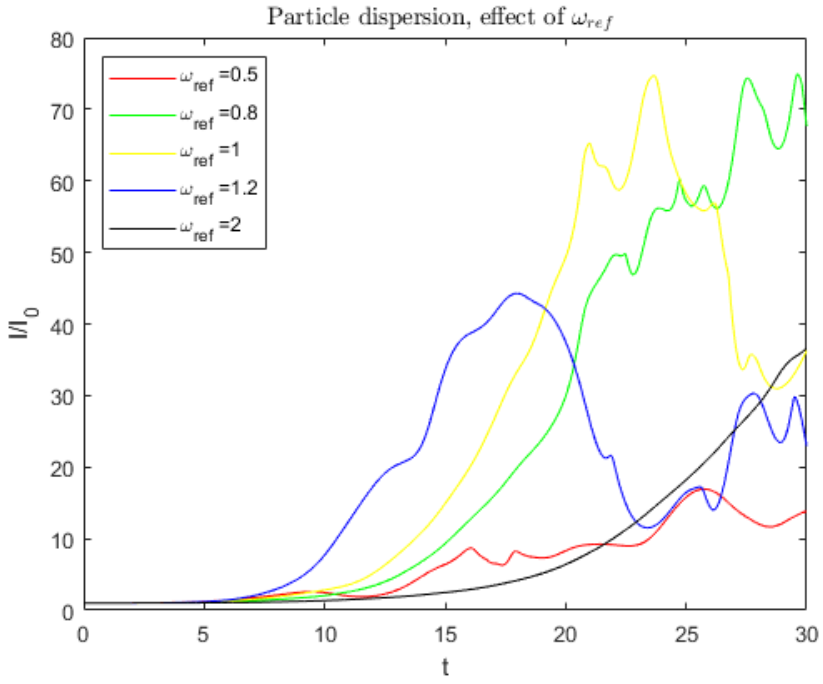

Figure 37: Indice di dispersione al variare di ω_{ref}.